Short communication

# Toward high specific capacity and high cycling stability of pure tin nanoparticles with conductive polymer binder for sodium ion batteries

CrossMark

Kehua Dai [a,b], Hui Zhao [b], Zhihui Wang [b], Xiangyun Song [b], Vince Battaglia [b], Gao Liu [b,*]

[a] School of Materials and Metallurgy, Northeastern University, Shenyang 110004, China
[b] Environmental Energy Technologies Division, Lawrence Berkeley National Laboratory, Berkeley, CA 94720, USA

## HIGHLIGHTS

- Pure Sn particle shows high specific capacity and high cycling stability with PFM conductive biner.
- The Sn/PFM electrode can deliver 806 mAh g$^{-1}$ at C/50 and 610 mAh g$^{-1}$ at C/10.
- After 10 cycles at C/10, the Sn/PFM electrode has no any capacity fading.

## ARTICLE INFO

## ABSTRACT

Pure Sn nanoparticles electrode with Poly(9,9-dioctylfluorene-co-fluorenone-co-methylbenzoic ester) (PFM) conductive binder was prepared and tested in sodium ion battery. It showed higher specific capacity and higher cycling stability without any carbon black compared with Sn/CMC (carboxy methylated cellulose) and Sn/PVDF (polyvinylidene fluoride) electrode. The Sn in Sn/PFM electrodes delivered 806 mAh g$^{-1}$ at C/50 and 610 mAh g$^{-1}$ at C/10. After 10 cycles at C/10, the capacity of Sn had no decay. SEM and TEM images showed that the Sn particles in Sn/PFM electrode were still in good conductive network despite big volume change, but parts of Sn particles in Sn/CMC or Sn/PVDF electrode are electrically isolated.

Published by Elsevier B.V.

## 1. Introduction

Recently, more and more attention has been paid to sodium ion batteries due to the wide availability and low cost of sodium [1,2]. There have been many kinds of cathode materials for sodium ion batteries [3–19]. However, it is still a huge challenge to develop a practical anode material with high specific capacity and high cycling stability. Graphite, which has been widely used in lithium ion batteries, does not work with sodium [20]. Although hard carbon can absorb Na atoms onto its surface thereby can be used as anode material for sodium ion batteries, its specific capacity (200–300 mAh g$^{-1}$) and density ($\sim$1.5 g cm$^{-3}$) are not satisfactory [20–23]. Metal oxide anode materials, such as sodium titanate or TiO$_2$, has lower specific capacity than hard carbon [24–32]. Intermetallic anode materials [33–38] (Si, Ge, Sn, Pb, Sb, etc.) have aroused much interest for their high specific capacity. Si has a high capacity of 4200 mAh g$^{-1}$ [39] but it also does not work in sodium ion batteries [40]. Thus, among the intermetallic anode materials for sodium ion batteries, Sn seems to be a competitive candidate [40–46]. The theoretical specific capacity of Sn is about 847 mAh g$^{-1}$ when assuming the full conversion into Na$_{15}$Sn$_4$ [43]. The density of β-Sn is 7.3 g cm$^{-3}$ so it also has high volumetric capacity. However, the pure Sn powder suffers from big volume change in charge and discharge [44], so it is a significant challenge to improve the cycling stability of pure Sn.

In our previous work on lithium ion batteries, we pointed out that the polymer binder plays an important role in the cell performance [47]. A conductive binder Poly(9,9-dioctylfluorene-co-fluorenone-co-methylbenzoic ester) (PFM) designed by our group has been used in Si and Sn anode material for lithium ion battery [48–50]. It is a polyfluorene-type polymer with two key function groups—carbonyl and methylbenzoic ester—for tailoring the

polymer to be conductive in the cycling potential range and for improving the mechanical binding force, respectively. With this binder, the pure Sn nanoparticles exhibit high cycling stability besides high specific capacity in lithium ion battery [49]. However, $Na^+$ has bigger ionic radius than $Li^+$, so the volume expansion of Sn during sodiation is bigger than during lithiation (430% [44] vs. 300% [49]). The PFM binder faces bigger challenge in the sodium system. In this work, we prepared Sn/PFM electrode without any conductive additive, then examined its electrochemical performance and compared it with Sn/CMC (carboxy methylated cellulose) and Sn/PVDF (polyvinylidene fluoride) electrode in the sodium-ion battery application.

## 2. Experimental

The detailed design, preparation, characterization and simulation of conductive polymer can be found in our published paper [50]. Sn nanoparticles were purchased from Sigma–Aldrich. The particle size defined by the company is <150 nm and the purity is over 99% by metal Sn content. Defined amount of Sn nanoparticles were dispersed in the conductive polymer PFM chlorobenzene solution to form a slurry. For comparison, the same Sn nanoparticles were also dispersed in CMC/water or PVDF/NMP solutions to form slurries. The slurries were doctor-bladed onto copper foil, dried at room temperature, then was punched into electrode discs with diameter of 12.7 mm. The electrodes were dried at 90 °C for 12 h in a vacuum oven. The weight ratios of Sn/PFM, Sn/CMC and Sn/PVDF were 95/5, 95/5 and 98/2, respectively. The mass loading of active materials of the three electrodes was about 1 mg, and the thickness was about 5 μm. 2325 coin cells were fabricated with the Sn electrodes, sodium foil, 1 mol $L^{-1}$ $NaClO_4$ in 7/3 (v/v) propylene carbonate (PC)/fluoroethylene carbonate (FEC), and two-layered Celgard 2400 polypropylene separator. The coin cells were assembled in an argon-filled glove box. Galvanostatic charge-discharge tests were performed using Maccor 4000 at 30 °C. The voltage range was 0.8–0.0001 V. The morphology of the electrodes was examined using a JEOL 7500F scanning electron microscope (SEM) and a Philips CM200FEG transmission electron microscopy (TEM).

## 3. Results and discussion

Fig. 1 shows the first charge and discharge profiles of the three electrodes. The charge capacities of Sn/PFM, Sn/CMC and Sn/PVDF are 806 mAh $g^{-1}$, 533 mAh $g^{-1}$, 65.7 mAh $g^{-1}$, respectively. Although PVDF is insulating, Sn is a highly conductive metal. In the pristine electrode, some particles are isolated by the coated PVDF, but other Sn particles are connected each other and with current collector due to agglomeration, so the Sn/PVDF electrode delivers 466 mAh $g^{-1}$ discharge capacity, which is 55% of the theoretical capacity of Sn (847 mAh $g^{-1}$). However, when the particles expand during sodiation, the distance of two particles center is also increase. When the cell starts charge, the particles shrink but the distance of two particles center remains due to the poor binding force of PVDF, so most of the particles are disconnected. Therefore, the Sn/PVDF electrode only delivers 65.7 mAh $g^{-1}$ charge capacity. On the other hand, the cutting of an electric conduction path of the electrodes may promote the decomposition of the electrolyte. As a result, it is possible to cause cycle degradation. The binding ability of CMC is far stronger than that of PVDF because its carboxylic groups can form hydrogen binding with Sn particles, so the connection of particles will not be affected significantly. However, the isolated particles will not be sodiated, so the Sn/CMC has the medium charge capacity (533 mAh $g^{-1}$). PFM has both high conductivity and high binding ability, thus despite some particles are physical isolated by PFM polymer, they are electrically connected. All the particles can be reversible sodiated/desodiated, so the Sn/PFM shows the highest charge capacity, which is close to the theoretical capacity of Sn. The charge profiles of Sn/PFM has four voltage plateaus: 0.13 V, 0.25 V, 0.56 V and 0.63 V, which refer to two-phase reactions of $Na_{15}Sn_4$–$Na_9Sn_4$, $Na_9Sn_4$–NaSn, NaSn–$NaSn_5$ and $NaSn_5$–Na, respectively [42–44,46]. The ration of plateau length is close to theoretical calculating value [41]. This suggests that the PFM binder holds the electrically connection during the whole sodiation and desodiaction process of Sn. The initial coulombic efficiency of Sn/PFM electrode is 70% due to the first discharge capacity is as high as 1150 mAh $g^{-1}$. The reason may be ascribed to some complicated side reaction. The actual reason and the way to improve still need further study.

Fig. 2 shows the cycling stability of the Sn/PFM, Sn/CMC and Sn/PVDF electrodes in sodium batteries. Firstly, at C/10, the initial charge capacity of Sn/PFM is 610 mAh $g^{-1}$, which is 75.7% of capacity at C/50, and is higher than previous result (less than 500 mAh $g^{-1}$, Sn 80%, carbon black 10%, PAA 10%, 50 mA $g^{-1}$ [40]). However, the ratios of capacities at C/10 and C/50 are only 63.6% and 5.3% for Sn/CMC and Sn/PVDF, respectively, so Sn/PFM shows the best rate performance. Secondly, the capacity of Sn/PFM is very stable along cycling. After 10 cycles, the charge capacity is still 621 mAh $g^{-1}$, and has no decay. Comparatively, the charge capacity of Sn/CMC decreases fast for the first 5 cycles then becomes stable
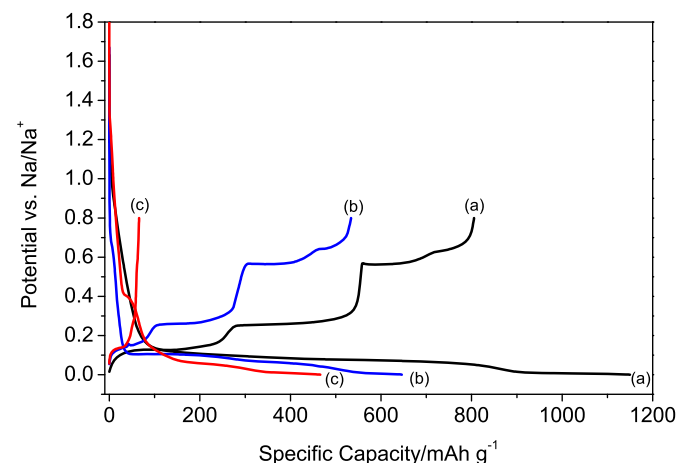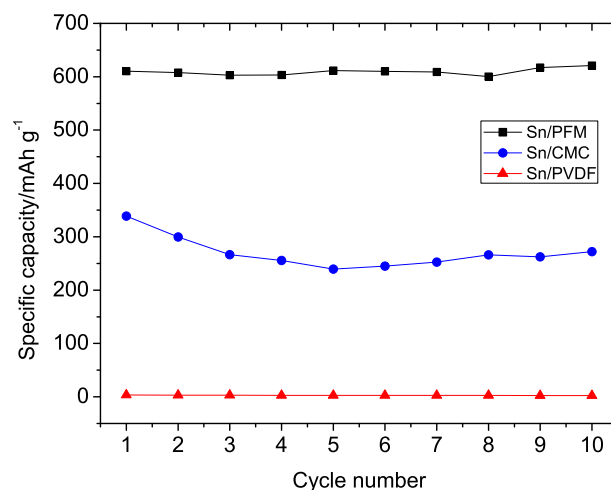


Fig. 1. The first charge and discharge voltage profiles of (a) Sn/PFM, (b) Sn/CMC and (c) Sn/PVDF electrodes. The charge and discharge rate is C/50 (16 mA $g^{-1}$, 0.012 mA $cm^2$).



Fig. 2. The charge capacity vs. cycle number of Sn/PFM, Sn/CMC and Sn/PVDF. The charge and discharge rate is C/10 (80 mA $g^{-1}$, 0.062 mA $cm^2$).
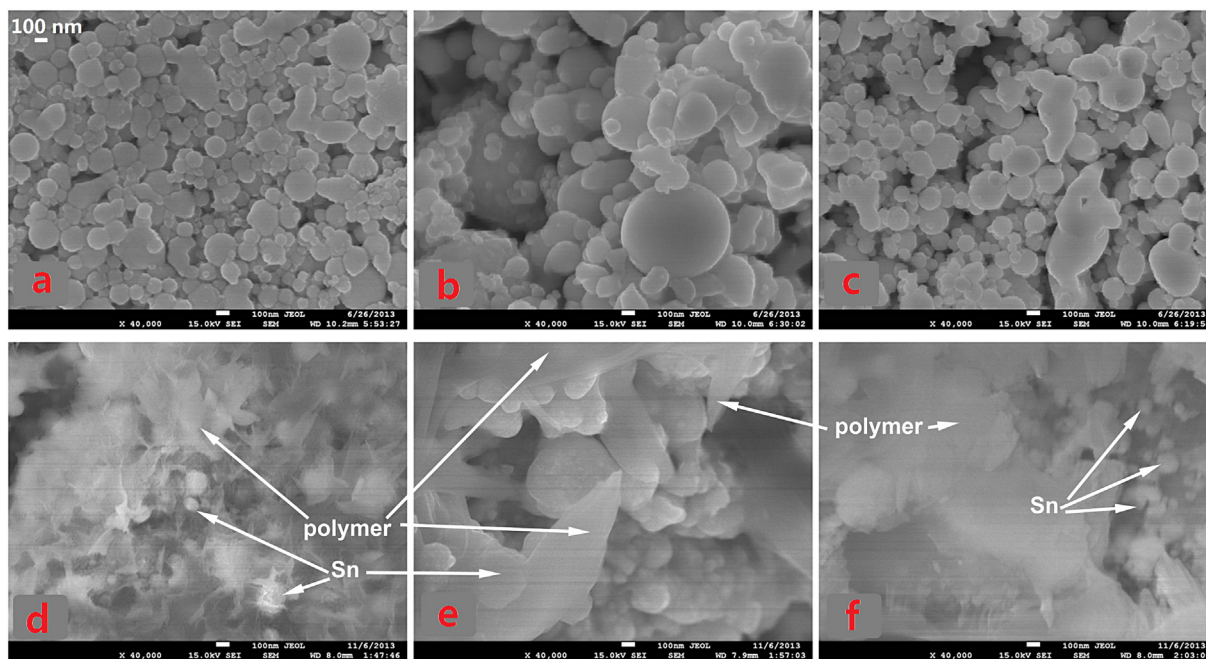
**Fig. 3.** SEM images of the three electrodes: (a) pristine Sn/PFM; (b) pristine Sn/CMC; (c) pristine Sn/PVDF; (d) Sn/PFM after 1 cycle; (e) Sn/CMC after 1 cycle; (f) Sn/PVDF after 1 cycle at C/50.

for the following 5 cycles. The capacity retention of Sn/CMC is only 80% after 10 cycles. The excellent cycling stability of Sn/PFM electrode in sodium ion battery is firstly ascribed to the good electrical conductivity and strong adhesion of PFM conductive binder.

Besides, the 30% FEC also has important effect on the performance of Sn electrodes [40,46]. Sakaguchi et al. suggest that FEC additive can effectively enhanced the utilization of active material by suppressing deterioration of the Na-ion transfer.
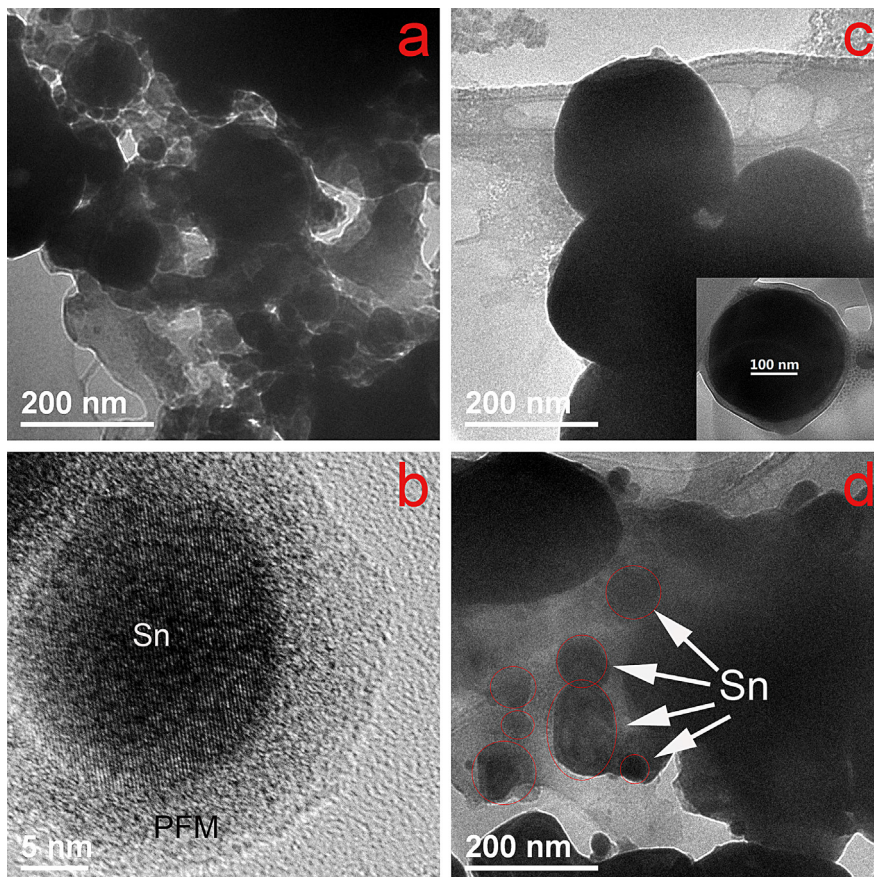


**Fig. 4.** TEM images of the electrodes: (a) (b) Sn/PFM after 1 cycle; (c) Sn/CMC after 1 cycle; (d) Sn/PVDF after 1 cycle at C/50.

Fig. 3 shows the morphology of the pristine and after-1-cycle electrodes. The three pristine electrodes of different composition have similar morphology, and polymer is hardly found in these images because all the polymer is uniformly coated onto the surface of particles. However, in the first cycle, because the Sn particles expand during sodiation and then shrink again during desodiation, the three electrodes after 1 cycle show much difference. The Sn particles in Sn/PFM electrode still bind closely to PFM polymer, but those in Sn/CMC and Sn/PVDF electrodes are separated from polymer. Sn particles in Sn/CMC electrode are still connected, but in Sn/PVDF electrode, some separated particles can be seen from Fig. 3f.

Fig. 4 is the TEM images of the three electrodes of different composition after 1 cycle. From (a) and (c) it can be seen that the Sn particles in Sn/PFM electrode are well connected by conductive binder to form an effective conductive network, and some particles in Sn/CMC are also connected tightly. However, many isolated Sn particles can be seen in the Sn/PVDF electrode (Fig. 4c). Fig. 4(b) shows high resolution image of a Sn particle in the Sn/PFM electrode after 1 cycle. The inner circle zone with lattice is Sn, and the outer ring zone without lattice is PFM polymer. The thickness of polymer is 7–9 nm, which agrees with our previous calculation [49]. Although the Sn particle is isolated by PFM polymer, electrons can still transfer between this particle and current collector through PFM conductive network. However, the Sn particles isolated by CMC in Fig. 4c and isolated by PVDF in Fig. 4d are not so lucky: they are electrically insulated so they cannot contribute capacity.

## 4. Conclusion

The electrode composed by pure Sn nanoparticles and PFM conductive polymer shows high specific capacity and high cycling stability without any conductive additive. The Sn in Sn/PFM electrodes delivers 806 mAh g$^{-1}$ at C/50 and 610 mAh g$^{-1}$ at C/10. After 10 cycles at C/10, the capacity of Sn has no decay. SEM and TEM images show that the Sn particles in Sn/PFM electrode are still in conductive network after huge expansion during sodiation and shrinkage during desodiation. This implies that the Sn electrode with PFM binder is a promising electrode for sodium ion batteries.

## Acknowledgment

## References

[1] M.D. Slater, D. Kim, E. Lee, C.S. Johnson, Adv. Funct. Mater. 23 (2013) 947–958.
[2] B.L. Ellis, L.F. Nazar, Curr. Opin. Solid State Mater. Sci. 16 (2012) 168–177.
[3] P. Barpanda, T. Ye, S. Nishimura, S.C. Chung, Y. Yamada, M. Okubo, H.S. Zhou, A. Yamada, Electrochem. Commun. 24 (2012) 116–119.
[4] N. Bucher, S. Hartung, I. Gocheva, Y.L. Cheah, M. Srinivasan, H.E. Hoster, J. Solid State Electrochem. 17 (2013) 1923–1929.
[5] K. Chihara, A. Kitajou, I.D. Gocheva, S. Okada, J. Yamaki, J. Power Sources 227 (2013) 80–85.
[6] J.J. Ding, Y.N. Zhou, Q. Sun, Z.W. Fu, Electrochem. Commun. 22 (2012) 85–88.
[7] J.J. Ding, Y.N. Zhou, Q. Sun, X.Q. Yu, X.Q. Yang, Z.W. Fu, Electrochim. Acta 87 (2013) 388–393.
[8] K.H. Ha, S.H. Woo, D. Mok, N.S. Choi, Y. Park, S.M. Oh, Y. Kim, J. Kim, J. Lee, L.F. Nazar, K.T. Lee, Adv. Energy Mater. 3 (2013) 770–776.
[9] Z.L. Jian, W.Z. Han, X. Lu, H.X. Yang, Y.S. Hu, J. Zhou, Z.B. Zhou, J.Q. Li, W. Chen, D.F. Chen, L.Q. Chen, Adv. Energy Mater. 3 (2013) 156–160.
[10] Z.L. Jian, H.J. Yu, H.S. Zhou, Electrochem. Commun. 34 (2013) 215–218.
[11] Z.L. Jian, L. Zhao, H.L. Pan, Y.S. Hu, H. Li, W. Chen, L.Q. Chen, Electrochem. Commun. 14 (2012) 86–89.
[12] J. Kang, S. Baek, V. Mathew, J. Gim, J. Song, H. Park, E. Chae, A.K. Rai, J. Kim, J. Mater. Chem. 22 (2012) 20857–20860.
[13] R. Kataoka, T. Mukai, A. Yoshizawa, T. Sakai, J. Electrochem. Soc. 160 (2013) A933–A939.
[14] S.W. Kim, D.H. Seo, X.H. Ma, G. Ceder, K. Kang, Adv. Energy Mater. 2 (2012) 710–721.
[15] M. Nose, S. Shiotani, H. Nakayama, K. Nobuhara, S. Nakanishi, H. Iba, Electrochem. Commun. 34 (2013) 266–269.
[16] J.F. Qian, X.Y. Wu, Y.L. Cao, X.P. Ai, H.X. Yang, Angew. Chem. Int. Ed. 52 (2013) 4633–4636.
[17] J.F. Qian, M. Zhou, Y.L. Cao, X.P. Ai, H.X. Yang, Adv. Energy Mater. 2 (2012) 410–414.
[18] P. Serras, V. Palomares, A. Goni, P. Kubiak, T. Rojo, J. Power Sources 241 (2013) 56–60.
[19] J.A. Saint, M.M. Doeff, J. Wilcox, Chem. Mater. 20 (2008) 3404–3411.
[20] D.A. Stevens, J.R. Dahn, J. Electrochem. Soc. 147 (2000) 1271–1273.
[21] R. Alcantara, J.M. Jimenez-Mateos, P. Lavela, J.L. Tirado, Electrochem. Commun. 3 (2001) 639–642.
[22] W. Luo, J. Schardt, C. Bommier, B. Wang, J. Razink, J. Simonsen, X.L. Ji, J. Mater. Chem. A 1 (2013) 10662–10666.
[23] A. Ponrouch, A.R. Goni, M.R. Palacin, Electrochem. Commun. 27 (2013) 85–88.
[24] Z.H. Bi, M.P. Paranthaman, P.A. Menchhofer, R.R. Dehoff, C.A. Bridges, M.F. Chi, B.K. Guo, X.G. Sun, S. Dai, J. Power Sources 222 (2013) 461–466.
[25] J.P. Huang, D.D. Yuan, H.Z. Zhang, Y.L. Cao, G.R. Li, H.X. Yang, X.P. Gao, RSC Adv. 3 (2013) 12593–12597.
[26] A. Rudola, K. Saravanan, S. Devaraj, H. Gong, P. Balaya, Chem. Commun. 49 (2013) 7451–7453.
[27] P. Senguttuvan, G. Rousse, V. Seznec, J.M. Tarascon, M.R. Palacin, Chem. Mater. 23 (2011) 4109–4111.
[28] Y. Sun, L. Zhao, H.L. Pan, X. Lu, L. Gu, Y.S. Hu, H. Li, M. Armand, Y. Ikuhara, L.Q. Chen, X.J. Huang, Nat. Commun. 4 (2013).
[29] W. Wang, C.J. Yu, Z.S. Lin, J.G. Hou, H.M. Zhu, S.Q. Jiao, Nanoscale 5 (2013) 594–599.
[30] W. Wang, C.J. Yu, Y.J. Liu, J.G. Hou, H.M. Zhu, S.Q. Jiao, RSC Adv. 3 (2013) 1041–1044.
[31] H. Xiong, M.D. Slater, M. Balasubramanian, C.S. Johnson, T. Rajh, J. Phys. Chem. Lett. 2 (2011) 2560–2565.
[32] Y. Xu, E.M. Lotfabad, H.L. Wang, B. Farbod, Z.W. Xu, A. Kohandehghan, D. Mitlin, Chem. Commun. 49 (2013) 8973–8975.
[33] L. Baggetto, E. Allcorn, R.R. Unocic, A. Manthiram, G.M. Veith, J. Mater. Chem. a 1 (2013) 11163–11169.
[34] L. Baggetto, J.K. Keum, J.F. Browning, G.M. Veith, Electrochem. Commun. 34 (2013) 41–44.
[35] M.K. Datta, R. Epur, P. Saha, K. Kadakia, S.K. Park, P.N. Kuma, J. Power Sources 225 (2013) 316–322.
[36] L. Wu, P. Pei, R.J. Mao, F.Y. Wu, Y. Wu, J.F. Qian, Y.L. Cao, X.P. Ai, H.X. Yang, Electrochim. Acta 87 (2013) 41–45.
[37] Y.H. Xu, Y.J. Zhu, Y.H. Liu, C.S. Wang, Adv. Energy Mater. 3 (2013) 128–133.
[38] T.T. Tran, M.N. Obrovac, J. Electrochem. Soc. 158 (2011) A1411–A1416.
[39] C.K. Chan, H.L. Peng, G. Liu, K. McIlwrath, X.F. Zhang, R.A. Huggins, Y. Cui, Nat. Nanotechnol. 3 (2008) 31–35.
[40] S. Komaba, Y. Matsuura, T. Ishikawa, N. Yabuuchi, W. Murata, S. Kuze, Electrochem. Commun. 21 (2012) 65–68.
[41] V.L. Chevrier, G. Ceder, J. Electrochem. Soc. 158 (2011) A1011–A1014.
[42] L.D. Ellis, T.D. Hatchard, M.N. Obrovac, J. Electrochem. Soc. 159 (2012) A1801–A1805.
[43] M. Mortazavi, J.K. Deng, V.B. Shenoy, N.V. Medhekar, J. Power Sources 225 (2013) 207–214.
[44] L. Baggetto, P. Ganesh, R.P. Meisner, R.R. Unocic, J.C. Jumas, C.A. Bridges, G.M. Veith, J. Power Sources 234 (2013) 48–59.
[45] H.L. Zhu, Z. Jia, Y.C. Chen, N. Weadock, J.Y. Wan, O. Vaaland, X.G. Han, T. Li, L.B. Hu, Nano Letters 13 (2013) 3093–3100.
[46] M. Shimizu, H. Usui, H. Sakaguchi, J. Power Sources 248 (2014) 378–382.
[47] G. Liu, H. Zheng, X. Song, V.S. Battaglia, J. Electrochem. Soc. 159 (2012) A214–A221.
[48] S.D. Xun, B. Xiang, A. Minor, V. Battaglia, G. Liu, J. Electrochem. Soc. 160 (2013) A1380–A1383.
[49] S.D. Xun, X.Y. Song, V. Battaglia, G. Liu, J. Electrochem. Soc. 160 (2013) A849–A855.
[50] G. Liu, S.D. Xun, N. Vukmirovic, X.Y. Song, P. Olalde-Velasco, H.H. Zheng, V.S. Battaglia, L.W. Wang, W.L. Yang, Adv. Mater. 23 (2011) 4679–4683.